PHENOMENOLOGICAL MODEL OF FILTRATION PROCESSES: 1. CAKE FORMATION AND EXPRESSION

R. BÜRGER[A,*], F. CONCHA[B], AND K.H. KARLSEN[C]

ABSTRACT. The phenomenological theory of sedimentation-consolidation processes of flocculated suspensions is extended to pressure filtration processes. The local mass and linear momentum balances for the solid and liquid component together with appropriate constitutive assumptions lead to a strongly degenerate (mixed hyperbolic-parabolic) nonlinear partial differential equation for the local solids fraction, which together with initial and boundary conditions determines a dynamic cake filtration process. In the case of a prescribed applied pressure function, we obtain a free boundary problem, in which the piston height has to be determined simultaneously with the solids concentration. A numerical algorithm approximating the physically correct solution, with possible discontinuities such as the cake/suspension interface, is presented and employed to simulate various cake filtration processes.

1. INTRODUCTION

Filtration is a process widely used in industry, especially in medicine and in chemical and mining as well as in food and paper companies. The variety of equipment and procedures that are utilized to filter the several materials in these industries is very large. For example, vacuum and pressure filtration is used in batch and continuous manner. Nevertheless the basic principles underlying filtration in all its diversity are the same. Filtration, as part of the more general field of solid-liquid separation, has its fundamentals in the flow of fluids in a porous medium and its quantification makes use, and abuse, of the famous Darcy equation (Darcy, 1856).

The scientific foundation of filtration was accomplished in the seventies by several groups of researchers in the Americas and in Europe. The development of the theory of filtration has its parallel in the formulation and application of the theory of thickening. For thickening, the phenomenological foundation was laid in the seventies and eighties (Concha and Bascur 1977, Concha and Bustos 1985, Buscall and White 1987, Auzerais et al. 1988), but the mathematical modelling and analysis and the design and application of suitable numerical methods have been performed only recently (Bustos et al. 1999, Bürger and Karlsen 2000a, Bürger et al. 2000b). In filtration, the flow in a rigid filter cake is well established and the case of a compressible cake is approximated by interpreting appropriately the same equations.

Date: September 24, 2000.

Key words and phrases. Filtration, numerical analysis, sedimentation, simulation, suspension, free boundary problem.

[a]Institute of Mathematics A, University of Stuttgart, Pfaffenwaldring 57, D-70569 Stuttgart, Germany, e-mail buerger@mathematik.uni-stuttgart.de.

[b]Department of Metallurgical Engineering, University of Concepción, Casilla 53-C, Correo 3, Concepción, Chile, e-mail fconcha@udec.cl.

[c]Department of Mathematics, University of Bergen, Johs. Brunsgt. 12, N-5008 Bergen, Norway, e-mail kenneth.karlsen@mi.uib.no.

[*]Corresponding author.

For this reason, filtration theory deals mainly with the conservation equations for the fluid, placing less attention to the behaviour of the solid. If a theory of filtration is aimed at, the deformation and motion of the solid should be included.

A second, and most important issue, in filtration theory is to recognize that the process is performed in stages, which do not necessarily involve the same fundamental principles. Take as an example the vacuum filtration in a rotary filter. Four stages can be observed: (1) a cake is formed by suctioning a suspension through a filter medium that retains the solid and lets the fluid pass; (2) the cake is dewatered by suctioning air through the pores, which replaces the liquid; (3) the cake is washed by suctioning water through the cake and (4) the cake is dehumidified by again suctioning air. In the case of pressure filtration, five stages can be distinguished: (1) a cake is formed by pressing a suspension through a filter medium; (2) the filter cake is compressed, reducing its porosity, by the direct contact with a solid surface, a mechanism known as expression; (3) dewatering is accomplished by blowing air through the cake; (4) water is pressed through the cake to wash it and (5) dehumidification is obtained by again blowing air through the cake.

In both cases, which represent the general trend in industrial solid-liquid filtration (see Massarani (1997), Wakeman and Tarleton (1999) and Rushton et al. (2000)), the cake formation and the expression eliminate most of the liquid from the suspension, leaving a saturated filter cake. These two steps are the simplest of the whole process because they involve the flow of only one fluid, the liquid, through the porous body formed by the consolidated particles. The principal variables are pressure, suspension concentration, temperature and time. These stages of pressure filtration can be analyzed by using a simple theory of flow through a porous medium. The dewatering and the washing stages in the filtration cycle are more complex. They should be analyzed as drainage or embedding of a liquid in a porous medium and, therefore, involve the flow of two fluids, a liquid and a gas, through the medium. In these stages, in addition to the previous variables, the saturation and the capillary pressure should be added. Saturation is the fraction of liquid filling the pores of the porous medium and capillary pressure is the pressure difference established between the air and the liquid when the first replaces the second from the filter cake. Capillary pressure and saturation are microscopic phenomena occurring within the porous medium and therefore they rarely appear in the macroscopic formulations of the filtration process we are accustomed to. It is evident that the foundation of these two last stages consists in the theory of two-phase flow through a porous medium, which will be topic of a future paper.

The aim of this first paper is to develop a theory for the cake formation and expression in the filtration process. It is organized as follows: In Section 2, we briefly specify the type of filtration process considered here. Section 3 is devoted to the development of the mathematical model. The local mass and linear momentum balances of the solid and of one fluid are recalled. Appropriate constitutive equations for the solid and fluid stresses and for the solid-fluid interaction force are established. Boundary conditions complement the resulting governing field equation for the solids concentration or equivalently, the porosity. The entire formulation leads to the concept of a *dynamic filtration process*, which from a mathematical point of view can be regarded as an initial-boundary value problem with a free boundary for one scalar strongly degenerate (or mixed hyperbolic-parabolic) convection-diffusion equation. In Section 4 we first mention some of the particular features of this highly nonlinear partial differential equation, whose solutions can be found only by numerical means. The mixed hyperbolic-parabolic nature of this equation implies that its solutions will typically be discontinuous and hence one has to be careful when designing numerical

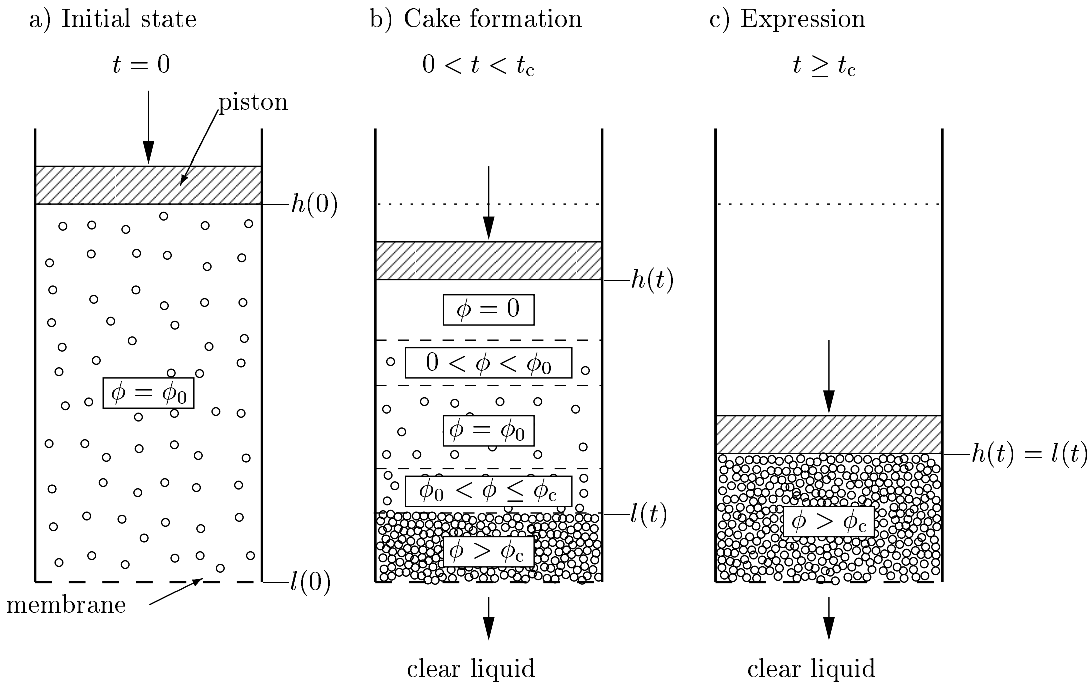

FIGURE 1. Steps in the pressure filtration of a flocculated suspension.

methods for computing them. Previous studies (Evje and Karlsen (2000)) have shown that numerical methods by based on naive finite difference discretization may fail to produce correct (i.e. physically relevant) solutions of strongly degenerate nonlinear partial differential equations. A suitable (i.e. working) numerical method for solving the mathematical model studied herein is introduced and numerical simulations of the cake filtration process are shown. A discussion of these results and an appropriate embedding of our model into the existing literature is provided in Section 5.

2. Physical model

Consider the pressure filtration of a suspension contained in the vessel with impervious and frictionless lateral walls shown in Figure 1. Pressure is exerted on the suspension from above, for example by a piston moving downwards, while the fluid is expelled from the bottom through a semi-permeable membrane, called filter medium. This medium can be a filter cloth or a membrane which has the property of retaining the solid while letting the fluid flow through. During pressure filtration five steps can be distinguished, the cake formation, the expression, dewatering, washing and the dehumidification of the filter cake by air blowing. The last three steps are not considered in this paper because they involve variables (saturation and capillary pressure) not yet considered in this formulation.

In the sequel, let ϕ denote the volumetric solids concentration, which is assumed to depend on the height z and on time t only. Before the filtration begins, the suspension is assumed to have a homogeneous volumetric solids concentration,

$$\phi(z,0) = \phi_0 \text{ for } 0 \le z \le h_0, \tag{1}$$

where $h_0 = h(0)$ is the initial height of the piston, see Figure 1 (a). During the step of cake formation two simultaneous processes may occur, the sedimentation of the suspension and the flow through the porous cake and filter medium at the bottom. In general, up to five different zones may be distinguished in the pressure vessel, see Figure 1 (b): At the top, a supernatant clear liquid zone may appear with $\phi = 0$. Below a transition zone where the concentration varies between zero and ϕ_0 may be distinguished. A zone of initial concentration $\phi = \phi_0$ follows and a new transition zone with $\phi_0 < \phi \leq \phi_{\mathrm{c}}$ may exist underneath, where ϕ_{c} is the critical concentration at which the solid flocs begin to touch each other. Finally, there is a fifth zone of consolidating porous cake with concentration equal or higher than ϕ_{c}. Whether sedimentation occurs or not depends, for a given material, on the initial concentration ϕ_0 and on the pressure exerted by the piston (or the blowing air that may substitute the piston) and consequently on the time involved on the filtration process. The cake formation time is usually so short that no significant sedimentation occurs.

3. Mathematical model

Sedimentation, centrifugation, consolidation and filtration form part of the more general field of solid-liquid separation processes of particulate systems. Therefore each of them should be considered as a special case of this general area of engineering science and their governing equations should stem from the same root, the mass and momentum balances for a particulate system. For sedimentation-consolidation such models have been presented by Concha et al. (1996), Bürger and Concha (1998), Bürger (2000) and Bürger et al. (2000c), and for centrifugation-consolidation, by Bürger and Concha (2000). Filtration is the typical case where a one-dimensional equation model of the flow in a porous medium is adequate. Nevertheless, if sedimentation-filtration or centrifugation-filtration should be treated in conjunction, it is necessary to start with the more general one-dimensional model of a compressible particulate process.

3.1. **Dynamic process for a particulate system.**

Consider a body of solid particles intimately mixed with a fluid under the following conditions:

(1) The solid particles are small with respect to the container and of the same density.
(2) The individual particles and the fluid are incompressible.
(3) The particles are completely flocculated at the beginning of the process.
(4) There is no mass transfer between the solid and the fluid.
(5) The only body force is gravity.
(6) The particles are contained in a vessel with impervious frictionless lateral walls and a semi-permeable bottom.

Such a system may be regarded as continuous media with two superimposed components obeying the following local mass and linear momentum equations (Bustos et al. 1999): the continuity equation of the solid,

$$\frac{\partial \phi}{\partial t} + \frac{\partial}{\partial z}(\phi v_{\mathrm{s}}) = 0, \tag{2}$$

where v_{s} denotes the solid phase velocity; the momentum balance of the solid,

$$\frac{\partial \sigma_{\mathrm{e}}(\phi)}{\partial z} = -\Delta \varrho g \phi + \frac{m_{\mathrm{d}}}{1-\phi}, \tag{3}$$

where $\sigma_{\mathrm{e}}(\phi)$ is the effective solid stress function, which is a given constitutive function, $\Delta\varrho := \varrho_{\mathrm{s}} - \varrho_{\mathrm{f}} > 0$ is the solid-fluid density difference, g the acceleration of gravity and m_{d} the solid-fluid dynamic interaction force. The mass balance equation of the mixture is

$$\frac{\partial q}{\partial z} = 0, \tag{4}$$

where $q := \phi v_{\mathrm{s}} + (1-\phi)v_{\mathrm{f}} \equiv v_{\mathrm{s}} - (1-\phi)v_{\mathrm{r}}$ is the volume average velocity of the mixture if v_{f} is the fluid phase velocity and $v_{\mathrm{r}} := v_{\mathrm{s}} - v_{\mathrm{f}}$ denotes the solid-fluid relative or drift velocity. The linear momentum balance equation of the fluid is

$$\frac{\partial p}{\partial z} = -\varrho_{\mathrm{f}} g - \frac{m_{\mathrm{d}}}{1-\phi}, \tag{5}$$

where p denotes the pore pressure. Equations (2) to (5) follow from the full mass and linear momentum balance equations for both components if advective acceleration terms are neglected and if the the solid and fluid phase pressures are expressed in terms of the pressures σ_{e} and p. For details concerning the derivation of these equations, we refer to Concha et al. (1996), Bürger (2000) and Bürger et al. (2000c). If discontinuities appear, equations (2) to (5) have to be replaced by jump conditions, which can be derived from the macroscopic balances (Bustos et al., 1999).

3.2. **Cake formation and expression.** As mentioned above, the cake formation stage consists in the simultaneous sedimentation of the suspension, consolidation of the sediment, and flow of filtrate through the filter cake and the filter medium. Since the development of each of these particular different operations has followed different approaches, we will at first respect the original formulations, and will unify them afterwards.

3.2.1. *Sedimentation of the suspension.* In the theory of sedimentation it is customary to use the Kynch batch flux density function

$$f_{\mathrm{bk}}(\phi) := -\frac{\Delta\varrho g \phi^2 (1-\phi)^2}{\alpha(\phi)}, \tag{6}$$

where the resistance coefficient $\alpha(\phi)$ is assumed to be a given function appearing in the constitutive relationship

$$m_{\mathrm{d}} = -\alpha(\phi) v_{\mathrm{r}}. \tag{7}$$

In view of equation (3), we obtain from (6)

$$\phi v_{\mathrm{s}} = q\phi + f_{\mathrm{bk}}(\phi)\left(1 + \frac{\sigma_{\mathrm{e}}'(\phi)}{\Delta\varrho g \phi}\frac{\partial \phi}{\partial z}\right). \tag{8}$$

Substituting this into (2) and taking into account (4), we obtain the known strongly degenerate parabolic equation describing the settling of flocculated suspensions (Bürger and Concha 1998):

$$\frac{\partial \phi}{\partial t} + \frac{\partial}{\partial z}\big(q(t)\phi + f_{\mathrm{bk}}(\phi)\big) = \frac{\partial}{\partial z}\left(-\frac{f_{\mathrm{bk}}(\phi)\sigma_{\mathrm{e}}'(\phi)}{\Delta\varrho g \phi}\frac{\partial \phi}{\partial z}\right). \tag{9}$$

Introducing the diffusion coefficient $a(\phi)$ and its primitive $A(\phi)$ by

$$a(\phi) := -\frac{f_{\mathrm{bk}}(\phi)\sigma_{\mathrm{e}}'(\phi)}{\Delta\varrho g \phi}, \quad A(\phi) := \int_0^{\phi} a(s)\,ds, \tag{10}$$

equation (9) can be shortly rewritten as

$$\frac{\partial \phi}{\partial t} + \frac{\partial}{\partial z}\big(q(t)\phi + f_{\mathrm{bk}}(\phi)\big) = \frac{\partial^2}{\partial z^2} A(\phi). \tag{11}$$

In addition, we obtain the following linear momentum balance of the fluid, which can be employed to calculate the pore pressure p a posteriori from the concentration distribution:

$$\frac{\partial p}{\partial z} = -\varrho_{\mathrm{f}} g - \frac{\Delta\varrho g \phi^2(1-\phi)}{f_{\mathrm{bk}}(\phi)} v_{\mathrm{r}} \tag{12}$$

To illustrate that (9) is of strongly degenerate parabolic type, we recall that it is usually assumed that $\sigma_{\mathrm{e}}(\phi)$ vanishes for concentration values $\phi \leq \phi_{\mathrm{c}}$, and that

$$\sigma_{\mathrm{e}}'(\phi) := \frac{d}{d\phi}\sigma_{\mathrm{e}}(\phi) > 0 \text{ for } \phi > \phi_{\mathrm{c}}. \tag{13}$$

A common equation for σ_{e} that has been used to fit experimental data for $\phi > \phi_{\mathrm{c}}$ is the power law

$$\sigma_{\mathrm{e}}(\phi) = \sigma_0\big((\phi/\phi_{\mathrm{c}})^K - 1\big) \tag{14}$$

with parameters $\sigma_0, K > 0$. Moreover, it is assumed in general (Kynch 1952) that the function $f_{\mathrm{bk}}(\phi)$ satisfies

$$f_{\mathrm{bk}}(0) = f_{\mathrm{bk}}(\phi_{\max}) = 0, \ \ f_{\mathrm{bk}}(\phi) < 0 \text{ for } 0 < \phi < \phi_{\max}, \ \ f_{\mathrm{bk}}'(0) < 0, \ \ f_{\mathrm{bk}}'(\phi_{\max}) \geq 0, \tag{15}$$

where $\phi_{\max}$ is the maximum solids concentration for the material considered. A widely used flux density function is the Maude and Whitmore generalization (Maude and Whitmore 1958) of the Richardson-Zaki flux density function (Richardson and Zaki 1954)

$$f_{\mathrm{bk}}(\phi) = u_\infty \phi (1-\phi)^C, \ \ u_\infty < 0, \ \ C > 1. \tag{16}$$

Combining the properties (15) of $f_{\mathrm{bk}}(\phi)$ and those of $\sigma_{\mathrm{e}}(\phi)$, we see that the diffusion coefficient $a(\phi)$ given by (10) vanishes for $\phi \leq \phi_{\mathrm{c}}$ and $\phi = \phi_{\max}$ and is positive for $\phi_{\mathrm{c}} < \phi < \phi_{\max}$. In other words, equation (9) is hyperbolic for or $\phi \leq \phi_{\mathrm{c}}$ and $\phi = \phi_{\max}$ and parabolic for $\phi_{\mathrm{c}} < \phi < \phi_{\max}$, where the location of the type change interface, at which $\phi = \phi_{\mathrm{c}}$ is valid, is unknown beforehand. Since equation (9) degenerates from parabolic to hyperbolic type on the interval of solution values $[0, \phi_{\mathrm{c}}]$ of positive length, it is called strongly degenerate or mixed hyperbolic-parabolic.

3.2.2. *Flow through the filter cake.* To analyze a flow through a porous medium, the concept of porosity $\varepsilon \equiv 1 - \phi$ is frequently used instead of the volumetric solids concentration. In terms of ε, the linear momentum equation of the fluid (5) takes the form

$$\frac{\partial p}{\partial z} = -\varrho_{\mathrm{f}} g - \frac{m_{\mathrm{d}}}{\varepsilon}. \tag{17}$$

We assume that the following Darcy equation is valid, which acts as a constitutive equation for the resistive force:

$$m_{\mathrm{d}} = -\frac{\mu_{\mathrm{f}}}{k(\varepsilon)} H(\varepsilon) v_{\mathrm{r}}, \tag{18}$$

where μ_{f} is the fluid dynamic viscosity and $k(\varepsilon)$ is the permeability of the porous medium. The function $H(\varepsilon)$ can be chosen in such a way that the resulting linear momentum equation for the very well known case of flow through a rigid porous medium is satisfied. In this case, we have $v_\mathrm{s} \equiv 0$ and hence $v_\mathrm{r} = -v_\mathrm{f}$ and $q = \varepsilon v_\mathrm{f}$. Substituting (18) into (17) yields

$$\frac{\partial p}{\partial z} = -\varrho_\mathrm{f} g - \frac{\mu_\mathrm{f}}{k(\varepsilon)} \frac{H(\varepsilon)}{\varepsilon^2} q.$$

Since the classic result is

$$\frac{\partial p}{\partial z} = -\varrho_\mathrm{f} g - \frac{\mu_\mathrm{f}}{k(\varepsilon)} q, \tag{19}$$

we see that $H(\varepsilon) = \varepsilon^2$. Consequently, from equation (5) we have

$$m_\mathrm{d} = -\frac{\mu_\mathrm{f}\varepsilon^2}{k(\varepsilon)} v_\mathrm{r} \tag{20}$$

and therefore

$$\frac{\partial p}{\partial z} = -\varrho_\mathrm{f} g - \frac{\mu_\mathrm{f}\varepsilon}{k(\varepsilon)} v_\mathrm{r}. \tag{21}$$

In filtration, equation (21) is frequently referred to (Tiller and Yeh 1987, Tiller and Hsyung 1993) as Darcy-Shirato equation (Shirato et al. 1969). It is usually stated in the form

$$\frac{\partial p_\mathrm{e}}{\partial z} = -\frac{\mu_\mathrm{f}\varepsilon}{k(\varepsilon)} v_\mathrm{r}, \tag{22}$$

where

$$p_\mathrm{e} := p - \varrho_\mathrm{f} g \big(h(t) - z\big) \tag{23}$$

is the excess pore pressure, that is the pore pressure in excess of the hydrostatic pressure.

Note that in view of $v_\mathrm{r} = (v_\mathrm{s} - q)/\varepsilon$, equation (21) can be rearranged to yield

$$\frac{\partial p}{\partial z} = -\varrho_\mathrm{f} g + \frac{\mu_\mathrm{f}\varepsilon}{k(\varepsilon)} \Big(\frac{1}{1-\varepsilon} f - q \Big), \tag{24}$$

where

$$f = \phi v_\mathrm{s} \equiv (1-\varepsilon) v_\mathrm{s} \tag{25}$$

denotes the total solids flux density. Rearranging equation (24), we obtain

$$q = \frac{1}{1-\varepsilon} f - \frac{k(\varepsilon)}{\mu_\mathrm{f}\varepsilon} \Big(\frac{\partial p}{\partial z} + \varrho_\mathrm{f} g \Big). \tag{26}$$

Equation (26) shows that the filtrate flow depends on the solid flux density in addition to the pressure gradient.

3.2.3. *Consistency between sedimentation and filtration formulations.* For the process of sedimentation, being in part responsible for the formation of the filter cake, the linear momentum balance for the fluid should be given by (12). In the filter cake, where $\phi > \phi_\mathrm{c}$ is valid, this equation should be equivalent to equation (24). Comparing the right-hand parts of both equations, we see that the permeability function $k(\varepsilon)$ is related to the Kynch batch flux density function $f_\mathrm{bk}(\phi)$ by (Bürger et al. 2000a)

$$f_\mathrm{bk}(\phi) = -\frac{k(\varepsilon)}{\mu_\mathrm{f}} \Delta\varrho g \phi^2 = -\frac{k(1-\phi)}{\mu_\mathrm{f}} \Delta\varrho g \phi^2. \tag{27}$$

Consequently, a constitutive equation $k = k(\varepsilon)$ for a porous medium determines the portion of the Kynch batch flux density function $f_\mathrm{bk}(\phi)$ for $\phi > \phi_\mathrm{c}$. The interrelation (27) is the key ingredient for the formulation of a unified mathematical model for pressure filtration. Provided that $f_{\mathrm{bk}}(\phi)$ satisfies (27), the field equations (9) and (12) provide all the information necessary for the calculation of the filtration process. Moreover, inserting

$$v_{\mathrm{r}} = \frac{f_{\mathrm{bk}}(\phi)}{\phi(1-\phi)}\left(1 + \frac{\sigma_{\mathrm{e}}'(\phi)}{\Delta\varrho g\phi}\frac{\partial\phi}{\partial z}\right), \tag{28}$$

into equation (12) we obtain

$$\frac{\partial p}{\partial z} = -\varrho(\phi)g - \frac{\partial\sigma_{\mathrm{e}}(\phi)}{\partial z}, \tag{29}$$

where $\varrho(\phi) = \varrho_{\mathrm{s}}\phi + \varrho_{\mathrm{f}}(1-\phi)$ is the local density of the mixture. Obviously, the pore pressure distribution $p = p(z,t)$ can be calculated a posteriori from the concentration distribution. Consequently, the only field equation which actually has to be solved is equation (9). The unknown flow rate $q = q(t)$ will be determined from a boundary condition, as shall be demonstrated below.

In view of this result, it should be mentioned that the constitutive equation for σ_{e} given by (14) is equivalent to the frequent constitutive assumption (Tiller and Leu 1980, Stamatakis and Tien 1991) that the local solids concentration in the cake is given by

$$\phi = \phi_{\mathrm{c}}\big(1 + (\sigma_{\mathrm{e}}/p_A)\big)^{\beta} \tag{30}$$

with material specific parameters p_A and $\beta > 0$ if we choose $\sigma_0 = p_A$ and $k = 1/\beta$. Equation (30) can be used to transform a similar approach for the local permeability

$$k = k_0\big(1 + (\sigma_{\mathrm{e}}/p_A)\big)^{-\delta} \tag{31}$$

with parameters $k_0, \delta > 0$ into values of $f_{\mathrm{bk}}(\phi)$, which yields

$$f_{\mathrm{bk}}(\phi) = -\frac{\Delta\varrho g k_0 \phi_{\mathrm{c}}^{\delta/\beta}}{\mu_{\mathrm{f}}}\phi^{2-\frac{\delta}{\beta}}. \tag{32}$$

Under most circumstances, however, we have $2 - \frac{\delta}{\beta} < 0$, so that the expression (32) is appropriate only where ϕ is bounded away from zero, which is the case under the restriction of formula (27) to $\phi > \phi_{\mathrm{c}}$.

3.3. **Boundary conditions and filtration rate.**

3.3.1. *Kinematic boundary conditions.* To obtain suitable boundary conditions, first note that (4) implies that

$$q = q(t) = h'(t) := \frac{dh(t)}{dt}. \tag{33}$$

In each mode of operation, the presence of the filter medium at $z = 0$ implies that no solids leave the filtration equipment, i.e.

$$v_{\mathrm{s}}|_{z=0} = 0. \tag{34}$$

Recalling from (10) the definitions of $a(\phi)$ and $A(\phi)$, we obtain from equation (8) the following boundary condition at $z = 0$:

$$\left(f_{\mathrm{bk}}(\phi) - \frac{\partial A(\phi)}{\partial z}\right)(0,t) = -h'(t)\phi(0,t), \quad t > 0. \tag{35}$$

The second boundary condition has to be prescribed at $z = h(t)$. Therefore we note that if the filtration rate is faster than the settling velocity,

$$v_{\mathrm{s}}|_{z=h(t)} = h'(t).$$

Inserting this into (8) yields

$$\left(f_{\mathrm{bk}}(\phi) - \frac{\partial A(\phi)}{\partial z}\right)(h(t),t) = 0, \quad t > 0. \tag{36}$$

3.3.2. *Coupling between applied pressure and filtrate flow rate.* Combined with the initial concentration distribution given by (1), conditions (35) and (36) yield an initial-boundary value problem (IBVP) for solving equation (9). However, the IBVP (1), (9), (35), (36) is of different character for both modes of operation.

To elucidate this argument, we now derive the coupling equation between the piston height $h(t)$ and the applied pressure $\sigma(t)$. To this end, first note that the sum of the momentum balance equations (3) and (5) yields the equation

$$\frac{\partial p_{\mathrm{t}}}{\partial z} = -\varrho(\phi)g, \tag{37}$$

where

$$p_{\mathrm{t}}(z,t) = p(z,t) + \sigma_{\mathrm{e}}\big(\phi(z,t)\big) \tag{38}$$

denotes the total pressure. Integrating (37) with respect to z and bearing in mind that the total pressure at piston height $z = h(t)$ is the applied pressure, i.e.

$$p_{\mathrm{t}}\big(h(t),t\big) = \sigma(t), \tag{39}$$

we see that at $z = 0$, the total pressure equals the applied pressure plus the weight of the solid and the fluid:

$$p_{\mathrm{t}}(0,t) = \sigma(t) + g\int_0^{h(t)} \varrho\big(\phi\,(\xi,t)\big)\,d\xi = \sigma(t) + g\big(m_0 - \varrho_{\mathrm{f}}\,(h_0 - h(t))\big), \tag{40}$$

where

$$m_0 = \int_0^{h_0} \varrho\big(\phi_0\,(\xi)\big)\,d\xi$$

denotes the total mass of suspension at $t = 0$. Inserting (40) into (38), we obtain

$$\sigma(t) = \sigma_{\mathrm{e}}\big(\phi(0,t)\big) - g\big(m_0 + \varrho_{\mathrm{f}}\,(h(t) - h_0)\big) + p(0,t). \tag{41}$$

3.3.3. *Filter medium resistance and final form of the coupling equation.* To determine the term $p(0,t)$ in equation (41), we consider the flow of the fluid through the filter medium. The thickness of the filter medium, h_{m}, is assumed to be very small. Therefore we denote by "0^+" values of a variable just above and by "0^-" just below the filter medium (Landman and Russel 1993). Darcy's law for the flow through the filter medium at $z = 0$ gives

$$-v_{\mathrm{f}}(0^-,t) = \frac{k_{\mathrm{m}}}{\mu_{\mathrm{f}}}\frac{\partial p}{\partial z}(0^-,t), \tag{42}$$

where k_{m} is the filter permeability. We may now approximate the derivative on the right-hand part of (42) by a difference quotient in order to obtain

$$-v_{\mathrm{f}}(0^-,t) = \frac{k_{\mathrm{m}}}{\mu_{\mathrm{f}} h_{\mathrm{m}}}\big(p(0^+,t) - p_{\mathrm{atm}}\big). \tag{43}$$

We can assume that the pressures are scaled in such a way that the atmospheric pressure p_{atm} is zero (Landman et al. 1991). We assume that the space immediately below the filter medium is entirely filled with fluid, i.e.

$$\phi(0^-,t)=0. \tag{44}$$

To ensure continuity of the liquid flow, we require that

$$\bigl(1-\phi(0^+,t)\bigr)v_{\mathrm{f}}(0^+,t)=\bigl(1-\phi(0^-,t)\bigr)v_{\mathrm{f}}(0^-,t). \tag{45}$$

In view of

$$\bigl(1-\phi(0^+,t)\bigr)v_{\mathrm{f}}(0^+,t)=h'(t), \tag{46}$$

we obtain from (44)–(46)

$$v_{\mathrm{f}}(0^-,t)=h'(t). \tag{47}$$

If we replace the ratio $k_{\mathrm{m}}/h_{\mathrm{m}}$ by the medium resistance R_{m} (Tiller and Yeh 1987, Font and Hernández 2000), we obtain by inserting (47) into (43) the desired coupling equation

$$\sigma(t)=\sigma_{\mathrm{e}}\bigl(\phi(0,t)\bigr)-g\bigl(m_0+\varrho_{\mathrm{f}}\,(h(t)-h_0)\bigr)-\mu_{\mathrm{f}}R_{\mathrm{m}}h'(t). \tag{48}$$

We finally mention that equation (48) coincides with the formulations by both Landman and Russel (1993) and Font and Hernández (2000). Equation (48) establishes the relationship between the pressure applied to the piston, $\sigma(t)$, and the filtrate flow rate or liquid expression rate $dh(t)/dt$. Since equation (48) involves the unknown solution value $\phi(0,t)$ and is essentially based on a force balance, we may refer to it as *dynamic boundary condition.*

3.4. **Dynamic cake filtration process.** Collecting the results, we can say that the sought variables, the concentration $\phi=\phi(z,t)$ (or, equivalently, the porosity $\varepsilon=\varepsilon(z,t)$ in a saturated medium), the pore pressure $p=p(z,t)$ and one of the two variables applied pressure $\sigma=\sigma(t)$ or filtrate flow rate $h'(t)\equiv q(t)$, are solution of a dynamic cake filtration process if they satisfy the field equations

$$\frac{\partial\phi}{\partial t}+\frac{\partial}{\partial z}\bigl(h'(t)\phi+f_{\mathrm{bk}}(\phi)\bigr)=\frac{\partial^2A(\phi)}{\partial z^2},\quad 0<z<h(t),\ t>0, \tag{49}$$

$$\frac{\partial p}{\partial z}=-\varrho(\phi)g-\frac{\partial\sigma_{\mathrm{e}}(\phi)}{\partial z},\quad 0<z<h(t),\ t>0, \tag{50}$$

where the function $A(\phi)$ is defined in (10). These field equations are considered together with the initial conditions

$$h(0)=h_0, \tag{51}$$

$$\phi(0,z)=\phi_0(z),\quad 0\le z\le h_0, \tag{52}$$

the kinematic boundary conditions

$$\left(f_{\mathrm{bk}}(\phi)-\frac{\partial A(\phi)}{\partial z}\right)(0,t)=-h'(t)\phi(0,t),\quad t>0, \tag{53}$$

$$\left(f_{\mathrm{bk}}(\phi)-\frac{\partial A(\phi)}{\partial z}\right)\bigl(h(t),t\bigr)=0,\quad t>0, \tag{54}$$

and the dynamic boundary condition

$$\sigma(t)=\sigma_{\mathrm{e}}\bigl(\phi(0,t)\bigr)-g\bigl(m_0+\varrho_{\mathrm{f}}\,(h(t)-h_0)\bigr)-\mu_{\mathrm{f}}R_{\mathrm{m}}h'(t). \tag{55}$$

The *material properties* of the suspension and the filter cake are represented by the Kynch batch flux density function $f_{\mathrm{bk}}(\phi)$, the effective solid stress function $\sigma_{\mathrm{e}}(\phi)$ and the constants $\Delta\varrho$ and μ_{f}. The *filtration equipment* is characterized by the initial height h_0 and the filter medium resistance. The *control functions* prescribed externally are either the applied pressure $\sigma(t)$ or the filtrate flow rate $h'(t)$.

3.5. **Modes of operation.** There are principally two different ways to operate the filter. Equations (53) and (55) play different roles in each of these modes of operation.

(1) *The rate of filtrate is a specified function of time.* In this case, the signed filtrate flow rate $dh(t)/dt$ is specified at all times, and the applied pressure $\sigma(t)$ has to be determined together with the solution of equation (49).

In this case, equations (49) to (54) form an initial-boundary value problem with a *moving boundary* $z = h(t)$, whose location is given a priori. This initial-boundary value problem can be solved for the concentration ϕ in a straightforward fashion, and the applied stress $\sigma(t)$ can be determined a posteriori by evaluating equation (55) using the calculated values of $\phi(0,t)$.

(2) *The applied piston pressure is a function of time.* In this more common case, the applied pressure $\sigma(t)$ is prescribed (for example, is assumed to be constant or is given by the pump flow rate), and the liquid expression rate $dh(t)/dt$ is determined with the solution. This case is more difficult since the unknowns $\phi(0,t)$ and $h'(t)$ appear in a nonlinear fashion in both conditions (53) and (55), and both quantities have to be determined simultaneously.

Transforming (53) into an ordinary differential equation for $h(t)$ and (55) into a boundary condition for $\phi(\cdot,t)$, we obtain

$$h'(t) = -\frac{1}{\phi(0,t)}\left(f_{\mathrm{bk}}\big(\phi(0,t)\big) - \frac{\partial A(\phi)}{\partial z}(0,t)\right), \quad t > 0 \tag{56}$$

and the Dirichlet boundary condition

$$\phi(0,t) = \sigma_{\mathrm{e}}^{-1}\Big(\sigma(t) + g\big(m_0 + \varrho_{\mathrm{f}}\,(h(t) - h_0)\big) + \mu_{\mathrm{f}} R_{\mathrm{m}} h'(t)\Big), \tag{57}$$

where σ_{e}^{-1} is the inverse function of $\sigma_{\mathrm{e}}(\phi)$ for $\phi > \phi_{\mathrm{c}}$. As mentioned above, the boundary $h(t)$ depends on $\sigma(t)$ and on the solution itself, therefore the initial-boundary value problem (49) to (55) is a problem with a *free boundary*, i.e. the upper boundary $h(t)$, the location of the piston at time t, is part of the solution. The second case is of course more difficult.

4. Numerical simulation of cake filtration processes

The equation describing the settling of flocculated suspensions (see (9)) is a highly non-standard partial differential equation. In particular, because of its nonlinear nature and mixed hyperbolic-parabolic type, solutions may become discontinuous even if the initial concentration is smooth. Consequently, the solutions have to be interpreted in a weak sense. However, weak solutions are not uniquely determined by their initial and boundary data, and additional selection criteria, or so-called entropy conditions, are needed to single out the unique physically relevant solution. We refer to Bürger and Karlsen (2000a), Bürger et al. (2000a,b) and to the lecture notes by Espedal and Karlsen (2000) (as well as the references cited in these papers) for details on the mathematical background of strongly degenerate nonlinear partial differential equations.

The nonlinear nature of mathematical model derived herein rules out analytical solution techniques and one has no other choice than resorting to numerical methods. When designing numerical methods for (9) one should be a bit careful. It was observed in Evje and Karlsen (2000) that numerical methods based on "naive" finite difference discretization may produce stable but physically wrong solutions. This feature is intimately connected to the fact that one has impose so-called entropy conditions in the continuous model to single out its unique physically relevant solution. Consequently, when designing numerical methods one has to make sure that the proposed methods has these entropy conditions or at least "discrete" versions of them "built in". As it is outside the scope of this paper to explain in detail why the numerical method described below produces correct solutions, let us simply say that this is (roughly speaking) related to the conservative form and the upwind nature of the method. In particular, the upwind nature implies that the method obeys a sort of discrete entropy condition. We refer to Bürger and Karlsen (2000a) and Bürger et al. (2000a,b), Evje and Karlsen (2000) and Karlsen and Risebro (2000) for details concerning the mathematical justification numerical method described below. For an overview of numerical methods for general degenerate partial differential equations, we refer again to the lecture notes by Espedal and Karlsen (2000).

4.1. **Numerical Algorithm.** For the numerical treatment it is convenient to transform the initial-boundary value problems to fixed height. To this end, we define the new coordinate $w = z/h(t)$. Noting that

$$\frac{\partial \phi}{\partial t}(z,t) = \frac{\partial \phi}{\partial t}(z,t) + \frac{\partial \phi}{\partial z}(z,t)\frac{dz}{dt} = \frac{\partial \phi}{\partial t}(w,t) - \frac{wh'(t)}{h(t)}\frac{\partial \phi}{\partial w}(w,t), \tag{58}$$

we obtain from (9)

$$\frac{\partial \phi}{\partial t} + \frac{h'(t)}{h(t)}(1-w)\frac{\partial \phi}{\partial w} + \frac{1}{h(t)}\frac{\partial f_{\mathrm{bk}}(\phi)}{\partial w} = \frac{1}{\big(h(t)\big)^2}\frac{\partial^2 A(\phi)}{\partial w^2}, \quad 0 \le w \le 1,\ t > 0. \tag{59}$$

The boundary conditions (35) and (36) take the respective forms

$$\left(f_{\mathrm{bk}}(\phi) - \frac{1}{h(t)}\frac{\partial A(\phi)}{\partial w}\right)(0,t) = -h'(t)\phi(0,t), \quad t > 0, \tag{60}$$

$$\left(f_{\mathrm{bk}}(\phi) - \frac{1}{h(t)}\frac{\partial A(\phi)}{\partial w}\right)(1,t) = 0, \quad t > 0, \tag{61}$$

and the initial condition (1) reads

$$\phi(w,0) = \phi_0(h(0)w,0), \quad 0 \le w \le 1. \tag{62}$$

It is now straightforward to adapt the upwind finite difference method developed for batch and continuous sedimentation of flocculated suspensions (Bürger and Karlsen 2000a) to the initial-boundary value problem given by equations (59) to (62). We refer to that paper (see also Bürger et al. 2000a,b) for details on the derivation of the method, its properties, and on the underlying mathematical background of degenerate hyperbolic-parabolic partial differential equations, and state here the resulting finite difference formulas concisely. To this end, divide the interval $[0,1]$ into J subintervals $[w_j, w_{j+1}]$ of length $\Delta w = 1/J$, where $w_j := j\Delta w$, $j = 0, \dots, J$.

Assume that an initial time step Δt^0 is given such that the stability condition

$$\frac{1}{h(t^n)}\Bigl(|h'(t^n)| + \max_{0\leq\phi\leq\phi_{\max}}\bigl|f_{\mathrm{bk}}(\phi)\bigr|\Bigr)\frac{\Delta t^n}{\Delta w} + \frac{2}{(h(t^n))^2}\max_{0\leq\phi\leq\phi_{\max}}|a(u)|\frac{\Delta t^n}{\Delta w^2} \leq 1-\epsilon, \quad n=0,1,2,\dots, \quad \epsilon>0 \tag{63}$$

is satisfied for $n=0$ with $t^0 := 0$.

The calculation starts by setting

$$\phi_j^0 := \phi_0\bigl(h(0)w_j\bigr), \quad j=0,\dots,J, \quad h^0 := h_0, \quad h^{-1} := h_0, \tag{64}$$

where ϕ_j^n denotes the approximate value of ϕ at $w=w_j$ and $t=t^n$, and similarly h^n is the approximate location of the free boundary, i.e. the piston height, at time t^n. Assume now that approximate solution values ϕ_j^n, $j=0,\dots,J$ and a value h^n for time t^n are known. If $t^n \geq T$, the calculation is stopped. Otherwise, a new time step Δt^n is determined from equation (63). We set $t^{n+1} := t^n + \Delta t^n$ and calculate ϕ_j^{n+1}, $j=0,\dots,J$, and a new height h^{n+1} from the following formulas:

- The solution value ϕ_0^{n+1} is directly prescribed by setting

$$\phi_0^{n+1} = \sigma_{\mathrm{e}}^{-1}\Bigl(\sigma\bigl(t^{n+1}\bigr) + g\bigl(m_0 + \varrho_{\mathrm{f}}(h^n - h_0)\bigr) + \mu_{\mathrm{f}}R_{\mathrm{m}}(h^n - h^{n-1})\Bigr). \tag{65}$$

- Calculate a new height h^{n+1} from

$$h^{n+1} = h^n - \frac{2\Delta t^{n+1}}{\phi_0^n + \phi_1^n}\biggl[f_{\mathrm{bk}}^{\mathrm{EO}}\bigl(\phi_0^n, \phi_1^n\bigr) - \frac{1}{\Delta t^{n+1}}\Bigl(A\bigl(\phi_1^n\bigr) - A\bigl(\phi_0^n\bigr)\Bigr)\biggr], \tag{66}$$

where the function $f_{\mathrm{bk}}^{\mathrm{EO}}(\cdot,\cdot)$ is the numerical flux function used by the scheme, namely the Engquist-Osher flux function (Engquist and Osher, 1981) defined by

$$f_{\mathrm{bk}}^{\mathrm{EO}}(u,v) := f_{\mathrm{bk}}(0) + \int_0^u \max\bigl\{0, f_{\mathrm{bk}}'(s)\bigr\}ds + \int_0^v \min\bigl\{0, f_{\mathrm{bk}}'(s)\bigr\}ds. \tag{67}$$

- To ensure second order accuracy in space of the method, we use the extrapolated variables

$$\phi_j^{n,\mathrm{L}} := \phi_j^n - \frac{\Delta w}{2}s_j^n, \quad \phi_j^{n,\mathrm{R}} := \phi_j^n + \frac{\Delta w}{2}s_j^n, \quad j=0,\dots,J, \tag{68}$$

where the slopes s_j^n are given by $s_0^n = s_1^n = s_{J-1}^n = s_J^n = 0$ and

$$s_j^n := \frac{1}{\Delta w}\mathrm{MM}\Bigl(\phi_j^n - \phi_{j-1}^n, \bigl(\phi_{j+1}^n - \phi_j^n\bigr)/2, \phi_{j+1}^n - \phi_j^n\Bigr), \quad j=2,\dots,J-2, \tag{69}$$

where the so-called minmod limiter function $\mathrm{MM}(\cdot,\cdot,\cdot)$ is given by

$$\mathrm{MM}(a,b,c) = \begin{cases} \min\{a,b,c\} & \text{if } a,b,c<0, \\ \max\{a,b,c\} & \text{if } a,b,c>0, \\ 0 & \text{otherwise.} \end{cases} \tag{70}$$

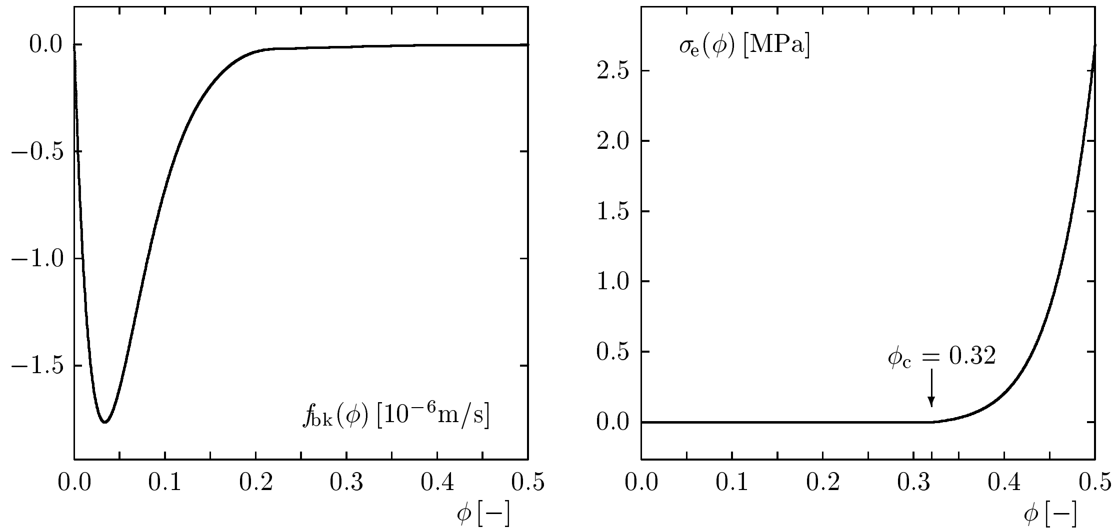

FIGURE 2. The constitutive functions f_{bk} (left) and σ_{e} (right) of the model suspension considered in the numerical examples.

The values ϕ_j^{n+1}, $j = 2, \dots, J-1$, are then calculated from the following interior scheme, which is a conservative finite difference discretization of equation (59):

$$\begin{aligned}\phi_j^{n+1} = \frac{h^n}{h^{n+1}}\biggl\{\phi_j^n - \frac{\Delta t^{n+1}}{h^{n+1}\Delta w}\biggl[\frac{h^{n+1}-h^n}{J\Delta t^{n+1}}\Bigl(\bigl(J-(j+1)\bigr)\phi_{j+1}^{n,\mathrm{L}} - \bigl(J-j\bigr)\phi_j^{n,\mathrm{L}}\Bigr)\\ + f_{\mathrm{bk}}^{\mathrm{EO}}\bigl(\phi_j^{n,\mathrm{R}}, \phi_{j+1}^{n,\mathrm{L}}\bigr) - f_{\mathrm{bk}}^{\mathrm{EO}}\bigl(\phi_{j-1}^{n,\mathrm{R}}, \phi_j^{n,\mathrm{L}}\bigr)\biggr]\\ + \frac{\Delta t^{n+1}}{(h^{n+1})^2\Delta w^2}\Bigl[A\bigl(\phi_{j+1}^n\bigr) - 2A\bigl(\phi_j^n\bigr) + A\bigl(\phi_{j-1}^n\bigr)\Bigr]\biggr\}, \quad j = 2, \dots, J-1.\end{aligned} \tag{71}$$

- Inserting the appropriate discrete analogue of boundary condition (60) into formula (71) for $j = 1$, we obtain the update formula for ϕ_1^n:

$$\begin{aligned}\phi_1^{n+1} = \frac{h^n}{h^{n+1}}\biggl\{\phi_j^n - \frac{\Delta t^{n+1}}{h^{n+1}\Delta w}\biggl[\frac{h^{n+1}-h^n}{J\Delta t^{n+1}}\Bigl((J-2)\phi_2^{n,\mathrm{L}} - (J-1)\phi_1^{n,\mathrm{L}}\Bigr)\\ + f_{\mathrm{bk}}^{\mathrm{EO}}\bigl(\phi_1^{n,\mathrm{R}}, \phi_2^{n,\mathrm{L}}\bigr) - f_{\mathrm{bk}}^{\mathrm{EO}}\bigl(\phi_0^{n,\mathrm{R}}, \phi_1^{n,\mathrm{L}}\bigr)\biggr] + \frac{\Delta t^{n+1}}{(h^{n+1})^2\Delta w^2}\Bigl[A\bigl(\phi_2^n\bigr) - A\bigl(\phi_1^n\bigr)\Bigr]\biggr\}.\end{aligned}$$

- Similarly, the appropriate discrete version of boundary condition (61) turns formula (71) for $j = J$ into an update formula for ϕ_J^n:

$$\phi_J^{n+1} = \frac{h^n}{h^{n+1}}\biggl\{\phi_J^n + \frac{\Delta t^{n+1}}{h^{n+1}\Delta w} f_{\mathrm{bk}}^{\mathrm{EO}}\bigl(\phi_{J-1}^{n,\mathrm{R}}, \phi_J^{n,\mathrm{L}}\bigr) - \frac{\Delta t^{n+1}}{(h^{n+1})^2\Delta w^2}\Bigl[A\bigl(\phi_J^n\bigr) - A\bigl(\phi_{J-1}^n\bigr)\Bigr]\biggr\}.$$

4.2. **Numerical examples.** The numerical algorithm was employed to simulate several dynamic cake filtration processes of a hypothetical suspension represented by the constitutive functions (see Fig. 2)

$$f_{\mathrm{bk}}(\phi)=\begin{cases} f_{\mathrm{bk}}^1(\phi) := -1.4073\times 10^{-4}\phi(1-\phi)^{28.875}\,\mathrm{m/s} & \text{if } 0<\phi\leq 0.14,\\ f_{\mathrm{bk}}^2(\phi) := -2.2522\times 10^{-11}\phi^{-5.\bar{1}}\,\mathrm{m/s} & \text{if } 0.32\leq\phi\leq\phi_{\max}:=0.5,\\ f_{\mathrm{bk}}^3(\phi) := f_{\mathrm{bk}}^2(0.32)+(\phi-0.32)\big(f_{\mathrm{bk}}^2\big)'(0.32) & \text{if } 0.22\leq\phi<0.32,\\ p_3(\phi) & \text{if } 0.14\leq\phi\leq 0.22,\\ 0 & \text{otherwise,}\end{cases} \tag{72}$$

where p_3 is the unique third-order polynomial defined on $[0.14, 0.22]$ which connects the segments f_{bk}^1 and f_{bk}^3 smoothly, and

$$\sigma_{\mathrm{e}}(\phi)=\begin{cases} 0 & \text{if } \phi\leq\phi_{\mathrm{c}}:=0.32,\\ 19000\big((\phi/\phi_{\mathrm{c}})^{11.\bar{1}}-1\big)\,\mathrm{Pa} & \text{if } \phi>\phi_{\mathrm{c}}.\end{cases} \tag{73}$$

The remaining parameters assumed to be constant in each example are $g=9.81\,\mathrm{m/s^2}$, $\Delta\varrho = 1618.18\,\mathrm{kg/m^3}$, $\mu_{\mathrm{f}}=0.000978\,\mathrm{Pa\,s}$, $h_0=0.094\,\mathrm{m}$ and $R_{\mathrm{m}}=3\times 10^{10}\,\mathrm{m^{-1}}$. The values of h_0, μ_{f} and R_{m} have been chosen in such a way that results can be compared with an experiment of pressure filtration of a kaolin suspension of initial concentration $\phi_0=0.03$, see Figure 8 of Tiller et al. (1995).

The first segment f_{bk}^1 of f_{bk} has been chosen according to the well-known Richardson and Zaki (1954) formula (16). The coefficient u_∞ and the exponent C have been chosen in such a way that settling rates observed with kaolin suspensions at the dilute initial concentrations 0.03 (Tiller et al. 1995) and 0.05 (Tiller et al. 1991) are well reproduced. The functions f_{bk}^3 and σ_{e} have been obtained from equations (30)–(32) using the parameters $p_A = 19000\,\mathrm{Pa}$, $\beta=0.09$, $\phi_{\mathrm{c}}=0.32$, $k_0=2.197\times 10^{-15}\,\mathrm{m^2}$ and $\delta=0.64$. Except for the value of k_0, these parameters were determined by Tiller and Horng (1983) (see also Tiller and Kwon (1998) and Tiller et al. (1999)) for kaolin. We first performed a calculation with the original value $\tilde{k}_0=1.09\times 10^{-14}\,\mathrm{m^2}$ published in these references. The result was that the simulated filtration rate was roughly twice as large as in the cited experiment of Tiller et al. (1995). Therefore we reduced the permeability of the sediment at given porosity, and thereby the filtration rate, by multiplying $\tilde{k}_0$ with a constant smaller than one. We found that the simulation reproduced the evolution of the measured piston height satisfactorily by choosing $k_0=0.43\tilde{k}_0$. It should be pointed out that Tiller et al. (1995) did not claim explicitly that the kaolin of their experiment was the same as that examined previously by Tiller and Horng (1983). Since published constitutive parameters for kaolin vary over large intervals (see e.g. Tiller et al., 1980, Wells 1999), the constitutive equations we finally utilized for this materials are not unreasonable.

The formation of and flow through the filter cake and the evolution of the free boundary $h(t)$ depend essentially on the portion of f_{bk} for $\phi>\phi_{\mathrm{c}}$, so results obtained from choosing different interpolations instead of that given by f_{bk}^3 and p_3, which has been designed on the consideration that the interpolant should not introduce additional extrema or inflection points, would look very similar to those presented below.

We mention that the function $A(\phi)$ has here the explicit representation

$$A(\phi)=\begin{cases} 0 & \text{for } \phi\leq\phi_{\mathrm{c}},\\ \dfrac{\sigma_0 k_0\beta\phi_{\mathrm{c}}^{(\delta-1)/\beta}}{\mu_{\mathrm{f}}(1-\delta)}\big(\phi^{(\beta-\delta+1)/\beta}-\phi_{\mathrm{c}}^{(\beta-\delta+1)/\beta}\big) & \text{for } \phi>\phi_{\mathrm{c}},\end{cases}$$

i.e. with the given parameters,

$$A(\phi) = \begin{cases} 0 & \text{for } \phi \leq 0.32, \\ 1.0176 \times 10^{-6}(\phi^5 - 0.003355443)\,\mathrm{m/s} & \text{for } \phi > 0.32. \end{cases}$$

Our simulation of the experiment of Tiller et al. (1995), where $\phi_0 = 0.03$, is shown in Figure 3: Fig. 3 (a) displays a filtration plot (similar to a settling plot) with measured and simulated iso-concentration lines, while Fig. 3 (b) shows the same numerical result as concentration profiles at selected times, together with concentrations at $\tilde{h}(t)$. As a consequence of the chosen parameters, the phenomenological model correctly predicts the movement of the piston. The formation and height of the filter cake are also well reproduced. The numerical simulation states that the bulk suspension of initial concentration ϕ_0 is always separated from the rising filter cake by a discontinuity, i.e. a concentration jump from 0.03 to $\phi_{\mathrm{c}} = 0.32$. This is not in agreement with the rising measured iso-concentration lines for the concentration values 0.029–0.031 and 0.05. The shape of the measured lines suggests that the discontinuity rising should be replaced by a continuous transition, at least between the concentrations 0.03 and 0.05, followed (from top to bottom) by a concentration discontinuity. To produce this effect, it would be necessary to modify the flux density function in the interval $[0.03, 0.05]$ such that a (lower) rarefaction wave replacing the rising discontinuity is produced (Bustos et al., 1999). Similarly, one could attempt to further modify the flux density function f_{bk} in such a manner that a concentration gradient forms between the piston (or a possible clear liquid supernate) and the bulk suspension, as suggested by the concept of upper rarefaction waves (Bürger and Tory, 2000). In other words, the main cause of the discrepancies between the measured data and the numerical simulation lies in the simple choice of the flux density function f_{bk} for $\phi \leq \phi_{\mathrm{c}}$, but not in the advanced theory of cake filtration.

In the remaining three examples we consider some hypothetical experiments by varying the initial concentration ϕ_0 and the applied pressure function $\sigma(t)$, but leave the remaining parameters unchanged.

We first choose the initial concentration $\phi_0 = 0.09$. Figure 4 (a) shows the simulated iso-concentration lines, and Figure 4 (b) displays the corresponding concentration profiles. In addition, and following the presentation of numerical results by Tiller and Yeh (1987), the concentration profile diagram (Fig. 4 (b)) displays the calculated concentration at piston height $\tilde{h}(t)$, plotted in time intervals of length $\Delta\tau$ (fat dots).

Figure 5 shows the simulated profiles of the excess pore pressure p_{e}, where this quantity has been normalized with respect to the maximum value $\sigma_{\max}$ of the applied pressure $\sigma(t)$. The profiles of p_{e} have been obtained from the calculated concentration distributions by the equation

$$\frac{\partial p_{\mathrm{e}}}{\partial z} = \Delta\varrho g\phi - \frac{\partial \sigma_{\mathrm{e}}(\phi)}{\partial z}, \quad 0 \leq z \leq h(t)$$

obtained from inserting (23) into (50). Furthermore, excess pore pressure values measured obtained in height $\tilde{h}(t)$ have been plotted into the p_{e} diagram, Fig. 5.

Figure 4 (a) shows that the filtration rate is decreasing while the filter cake is accumulating, and remains (nearly) constant when the cake is formed. At about $t = 4300\,\mathrm{s}$, the filtration stage is terminated, and the piston gets into contact with the filter cake. The cake is compressed in a very short time interval and assumes constant porosity.

The excess pore pressure diagram, Figure 5, illustrates that the excess pore pressure distribution remains constant while the filtration rate is constant, as expressed by the practical a)

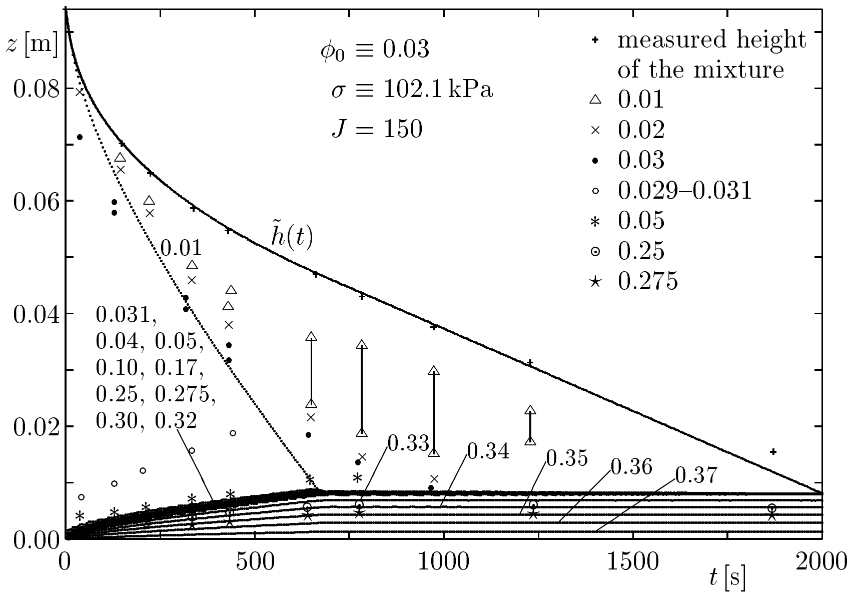

b)

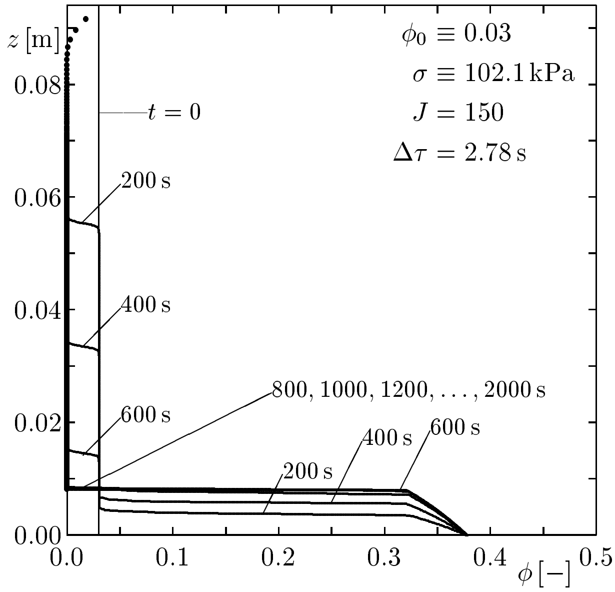

FIGURE 3. Simulation of a filtration experiment by Tiller et al. (1995): (a) filtration plot showing measured (symbols) and simulated iso-concentration lines corresponding to the annotated values, (b) simulated concentration profiles at selected times and concentrations (fat dots) at $\tilde{h}(t)$, plotted in time intervals of length $\Delta\tau$.

coincidence of the simulated p_{e} profiles for $t = 2500$, 3000, 3500 and 4500s. We also observe that the maximum excess pore pressure value, attained at the top of the filter cake, diminishes very rapidly once the piston height has attained the cake surface level.

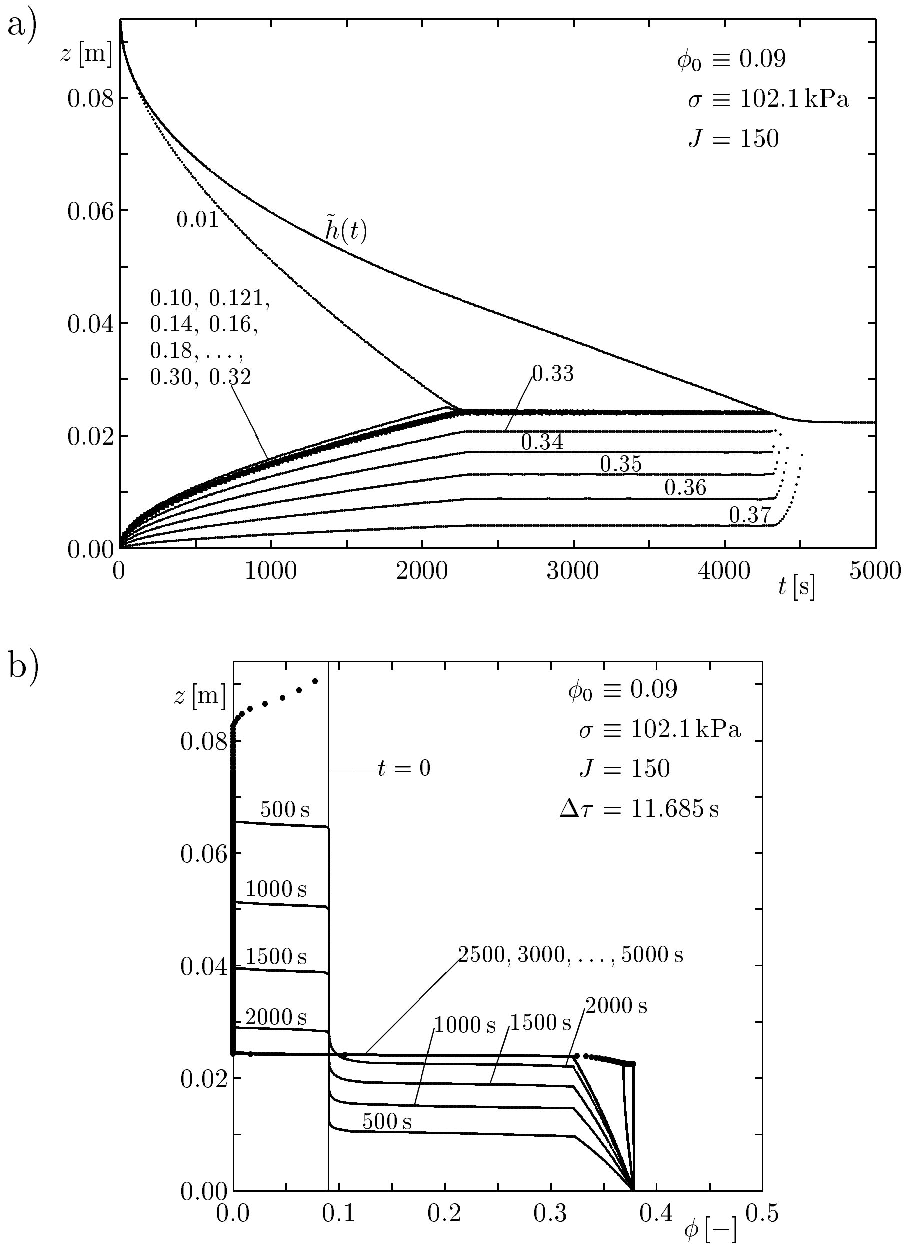

FIGURE 4. Simulation of pressure filtration of a concentrated suspension with $\phi_0 = 0.09$ and constant applied pressure $\sigma \equiv 102.1\,\mathrm{kPa}$: (a) filtration plot with simulated iso-concentration lines, (b) concentration profiles. The fat dots denote the concentration at height $\tilde{h}(t)$ and have been plotted in time intervals of length $\Delta\tau$.

Figures 6 and 7 show a simulation with the same initial concentration, $\phi_0 \equiv 0.09$, but with the non-constant, increasing applied pressure function

$$\sigma(t) = \begin{cases} 102.1\,\mathrm{kPa} & \text{for } 0 < t \leq 1000\,\mathrm{s}, \\ 200\,\mathrm{kPa} & \text{for } 1000\,\mathrm{s} < t \leq 2000\,\mathrm{s}, \\ 300\,\mathrm{kPa} & \text{for } 2000\,\mathrm{s} < t \leq 3000\,\mathrm{s}, \\ 400\,\mathrm{kPa} & \text{for } t > 3000\,\mathrm{s}. \end{cases} \tag{74}$$

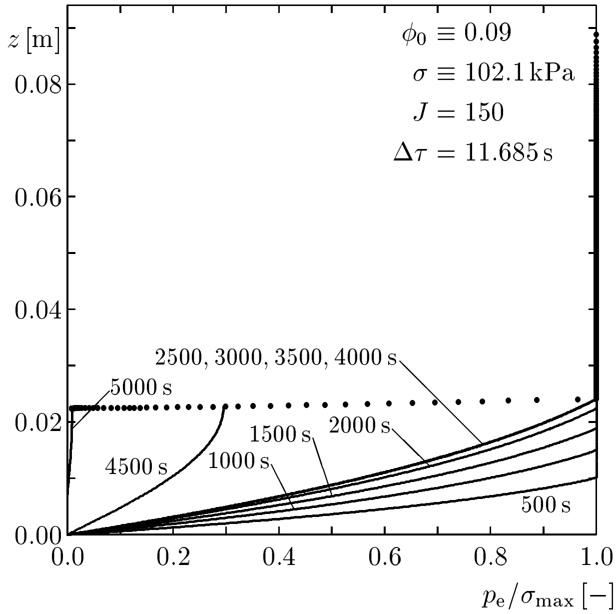

FIGURE 5. Excess pore pressure profiles corresponding to the simulation of Figure 4. The fat dots denote the excess pore pressure at height $\tilde{h}(t)$ and have been plotted in time intervals of length $\Delta\tau$.

To demonstrate the effect of successively increasing the applied pressure, the filtration plot, Figure 6 (a), also shows (as dashed lines, from top to bottom) the piston level curves that would have been obtained if the applied pressure had been kept constant at 102.1 kPa, if it had been changed at $t = 1000\,\mathrm{s}$ only, and if it had been changed at $t = 1000\,\mathrm{s}$ and $t = 2000\,\mathrm{s}$ only, respectively. Comparison with the calculated curve $\tilde{h}(t)$ produced by the function given by (74) clearly shows that each increment of the applied pressure function produces an increase of the filtrate flow rate. In addition, we observe that each of these steps produces an immediate increase of the concentration at $z = 0$, which is of course a consequence of equation (57). A similar direct consequence of (74) is expressed by the excess pore pressure profile plot for this example as shown in Figure 7.

In the last numerical example (Figures 8 and 9), we choose $\phi_0 = \phi_\mathrm{c} = 0.32$, i.e. the suspension is initially networked, and let $\sigma \equiv 200\,\mathrm{kPa}$. With these parameters, no hindered settling or clear liquid zones form, and the filtration process already starts with the expression stage. Although our parameters were chosen differently, our numerical results look similar to those displayed in Figures 14 and 15 of Tiller and Yeh (1987), Figure 9 of La Heij et al. (1996) Figures 6 and 7 of Sørensen et al. (1996).

5. CONCLUSIONS

We have shown in this paper how the existing theory of sedimentation-consolidation processes of flocculated suspensions can be extended to a phenomenological theory of cake filtration. The essential ingredients of this extension are an additional transport term in the known parabolic degenerate sedimentation-consolidation equation plus a coupling equation relating

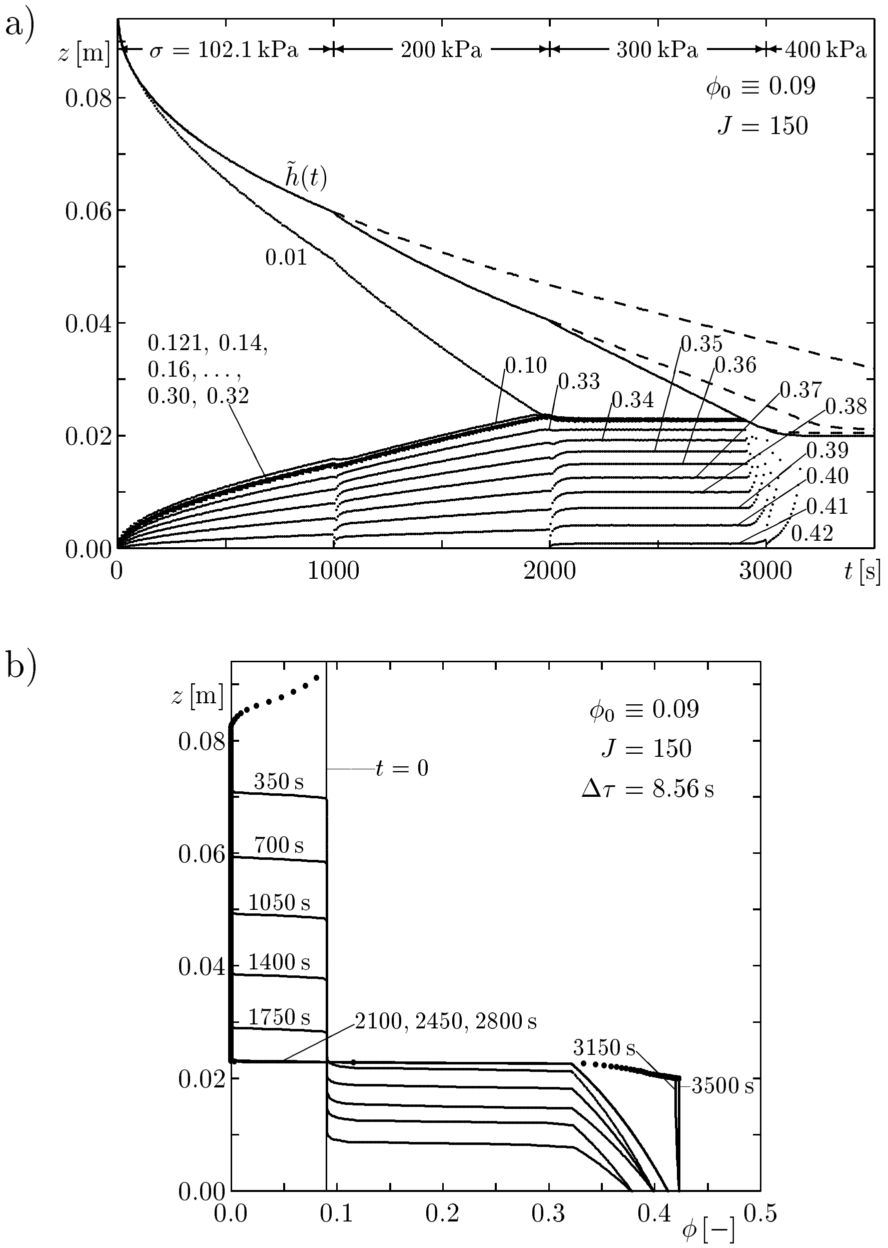

FIGURE 6. Simulation of pressure filtration of a concentrated suspension with $\phi_0 = 0.09$ and piecewise constant, increasing applied pressure function $\sigma(t)$: (a) filtration plot with simulated iso-concentration lines, (b) concentration profiles. The dashed lines correspond (from top to bottom) to piston heights calculated without increasing $\sigma(t)$ at all, after $t = 1000\,\mathrm{s}$, and after $t = 2000\,\mathrm{s}$, respectively. The fat dots denote the concentration at height $\tilde{h}(t)$ and have been plotted in time intervals of length $\Delta\tau$.

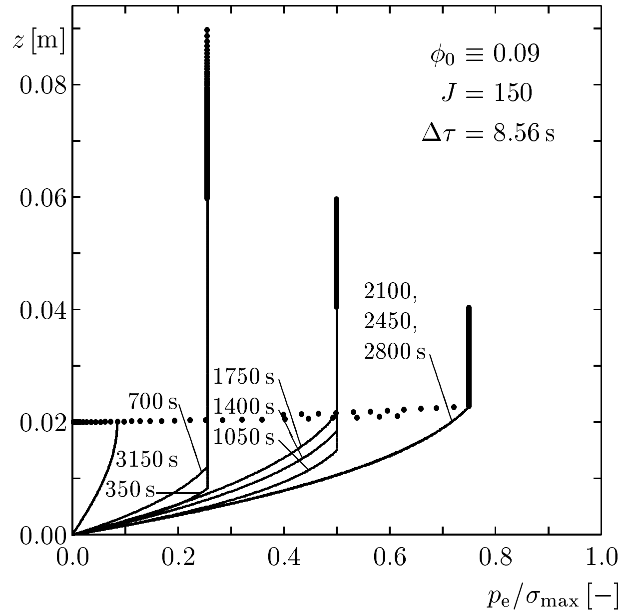

FIGURE 7. Excess pore pressure profiles corresponding to the simulation of Figure 6. The fat dots denote the excess pore pressure at height $\tilde{h}(t)$ and have been plotted in time intervals of length $\Delta\tau$.

the piston movement, or equivalently the volumetric flow rate, to the applied pressure. This coupling condition is essentially based on a balance of the total pressure.

We point out that theories of sedimentation, which are mostly based on the pioneering paper by Kynch (1952), rely on the solids concentration as independent variable, while the traditional filtration theory is based on the solids pressure, which is represented here by the concept of effective solid stress. However, since it is usually assumed that the concentration (or porosity) is a monotonous function of the solids stress wherever this quantity does not vanish, it is easily possible to refer filtration theory to the solids concentration as independent variable. As a consequence of this reformulation, the permeability now becomes a porosity-dependent function, and comparison with the sedimentation equations shows how the permeability equation has to be combined with known constants in order to form the portion of the flux density function for the compression zone.

The present formulation and the corresponding numerical method have some decisive advantages as compared to alternate treatments. It is possible to solve the free-boundary problem, and thereby to simulate the filtration process, explicitly without having to trace explicitly any of the interfaces (such as the cake/suspension and possibly the suspension/supernate interfaces) that may form in the interior of the computational domain. This is due to the fact that the numerical method approximates discontinuities in their correct locations, although they may be smeared out due to numerical diffusion, and is in contrast to more complicated treatments such as that by Sørensen et al. (1996), in which the cake/suspension interface gives rise to a moving boundary condition. The conservative form of the numerical algorithm ensures that the total amount of solids in the filter will remain constant during simulation (this is true, of course, up to roundoff errors). Moreover, due to the upwind nature of the

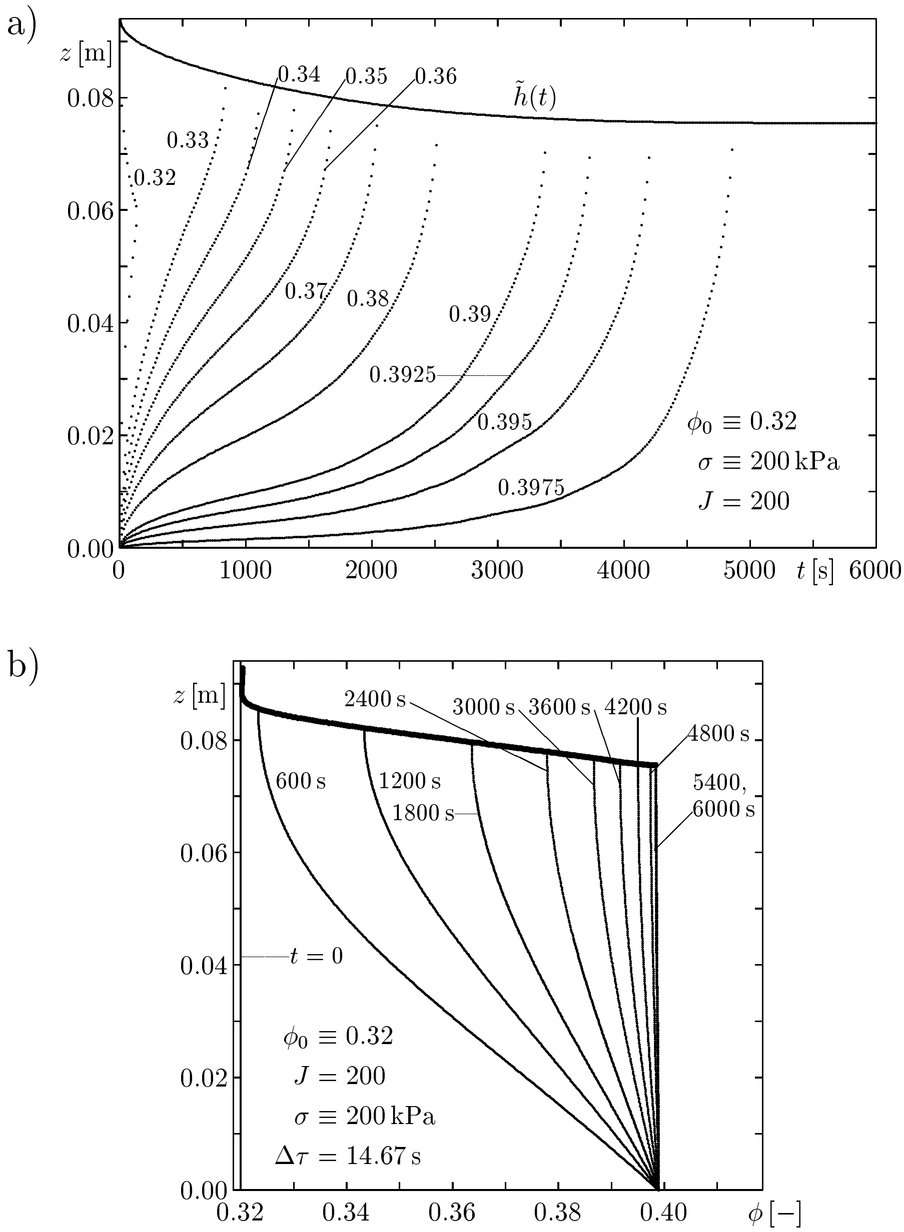

FIGURE 8. Simulation of pressure filtration of a concentrated suspension with $\phi_0 = \phi_c = 0.32$ and constant applied pressure $\sigma \equiv 200\,\text{kPa}$: (a) filtration plot with simulated iso-concentration lines, (b) concentration profiles. The fat dots denote the concentration at height $\tilde{h}(t)$ and have been plotted in time intervals of length $\Delta\tau$.

algorithm, it can be shown that only such discontinuities are approximated which are physically admissible, i.e. which satisfy a selection principle or entropy condition (Evje and Karlsen (2000) and Karlsen and Risebro (2000)). The related concept of entropy solutions and existence and uniqueness theory of degenerate parabolic equations has been fully developed for

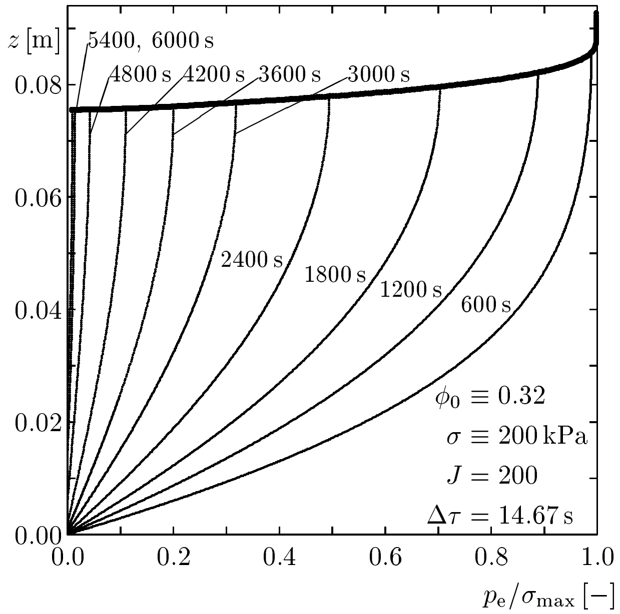

FIGURE 9. Excess pore pressure profiles corresponding to the simulation of Figure 8. The fat dots denote the excess pore pressure at height $\tilde{h}(t)$ and have been plotted in time intervals of length $\Delta\tau$.

the cases of gravity settling, continuous thickening and centrifugation of suspensions (Bürger et al. (2000b), Bürger and Karlsen (2000a,b)), and is currently being extended to the present free boundary problem (Bürger and Karlsen 2000c). The most obvious benefits for the practitioner that accrue from the mathematical analysis include here the well-posedness of the dynamical cake filtration process and the design of a numerical method for its computation.

To put the present work in the proper perspective, we mention that one of the first investigations of the effect on sedimentation on filtration of suspensions was undertaken by Straumann (1963), who, however, considered incompressible filter cakes only, which correspond here to the assumption that $\sigma_e \equiv 0$ and hence $a \equiv 0$, $A \equiv 0$. The present model is comparable to those formulated by Stamatakis and Tien (1991) and Font and Hernández (2000). However, Stamatakis and Tien (1991) do not include the effect of sedimentation and they assume that it is the suspension-cake interface where the prescribed pressure is applied, while in our work that interface is a result of the computation. Since the initial cake thickness is zero, Stamatakis and Tien (1991) have to formulate a separate procedure to initiate the numerical solution. Since it is assumed that the suspension concentration is uniform, as well as that the solids concentration always equals the critical, it is not clear to us how their approach can be extended to the expression stage. Similarly, the cake/suspension interface boundary condition derived by Atsumi and Akiyama (1975) is based on the assumption that the void ratio (or, equivalently, the concentration) of the suspension above the filter cake level is given by the initial value. To our view, this assumption is overly restrictive since it precludes that the slurry concentration directly above the cake may vary, which may occur due to prescribing non-constant initial data or due to the formation of rarefaction waves, as visible by characteristics (iso-concentration lines) emerging tangentially from the cake surface in a filtration plot. Such tangential characteristics may be produced by considering different shapes of the flux density function f_{bk} and selecting parameters appropriately, and their existence is even explicitly postulated in Font and Hernández' (2000) basic assumptions.

In the future, the numerical method should be employed to compare the predictions of the phenomenological model with experimental data, following the papers of Bürger et al. (2000a) and Garrido et al. (2000) for the case of gravity settling in a closed column. Published experimental studies that can be utilized for this purpose include the papers by Sambuichi et al. (1982), Zydney et al. (1989), Shen et al. (1994), Lu et al. (1998), Alles and Anlauf (1998), Wells (1999), Sis and Chander (2000), Font and Hernández (2000) and França (2000).

Combining the present work with that on centrifugation of flocculated suspensions (Bürger and Concha, 2000), it should be possible to extend the present phenomenological theory to filtering centrifuges. This will lead to a unified theory of solid-liquid separation processes, completing the work by Tiller and Hsyung (1993) and providing a formal mathematical background to that of Landman and White (1994), which can be employed for accurate design calculations.

Acknowledgements

Preparation of this work was made possible through the Applied Mathematics in Industrial Flow Problems (AMIF) programme of the European Science Foundation (ESF); through the Sonderforschungsbereich 404 at the University of Stuttgart; and through Fondef project D97-I2042 at the University of Concepción.

Notation

Latin symbols.

a	diffusion coefficient
A	integrated diffusion coefficient
C	exponent of the Richardson-Zaki flux density function
f	total solids flux density
f_{bk}	Kynch batch flux density function
$f_{\mathrm{bk}}^1, f_{\mathrm{bk}}^2, f_{\mathrm{bk}}^3$	segments of f_{bk}
$f_{\mathrm{bk}}^{\mathrm{EO}}$	Engquist-Osher flux function
g	acceleration of gravity
h	piston height
$\tilde{h}$	numerically calculated value of h
h_0	initial piston height
h_{m}	filter medium thickness
H	auxiliary function introduced in equation (18)
J	number of spatial subintervals
k	permeability
k_0	coefficient in the permeability equation (31)
$\tilde{k}_0$	published value of k_0 for kaolin
k_{m}	filter medium permeability
K	exponent in effective solid stress function
m_0	total mass of suspension at $t=0$
m_{d}	solid-fluid dynamic interaction force
MM	minmod limiter function

n	time step counter
p	pore pressure
p_3	third-order interpolation polynomial
p_A	parameter in the effective solid stress equation (30)
p_{atm}	atmospheric pressure
p_{e}	excess pore pressure
p_{t}	total pressure
q	volume average velocity of the mixture
R_{m}	filter medium resistance
s_j^n	slopes in numerical method
t	time
t^n	time after n iterations
u_∞	coefficient of the Richardson-Zaki flux density function
v_{f}, v_{s}	solid and fluid phase velocities
v_{r}	solid-fluid relative velocity
w	scaled height variable
z	height

Greek symbols.

α	resistance coefficient
β	exponent in the effective solid stress equation (30)
δ	exponent in the permeability equation (31)
Δt^n	time step
Δw	spatial meshwidth in numerical method
$\Delta \varrho$	solid-fluid density difference
$\Delta \tau$	plot interval in profile diagrams
ε	porosity
ϵ	positive constant in inequality (63)
ϕ	volumetric solids concentration
ϕ_0	initial concentration
ϕ_{c}	critical concentration
ϕ_j^n	approximate value of ϕ
$\phi_j^{n,\mathrm{L}}$, $\phi_j^{n,\mathrm{R}}$	extrapolated variables
$\phi_{\max}$	maximum concentration
μ_{f}	fluid dynamic viscosity
ϱ	local density of the mixture
ϱ_{s}, ϱ_{f}	solid and fluid mass densities
σ	applied pressure
σ_0	coefficient in effective solid stress function
σ_{e}	effective solid stress
σ_{e}^{-1}	inverse function of $\sigma_{\mathrm{e}}(\phi)$ for $\phi > \phi_{\mathrm{c}}$

References

Alles, C., Anlauf, H. 1998. Zur Wahl des Filtrationsdruckes bei der Filtration mit kompressiblen Kuchen. Chem.-Ing.-Techn., 70, 1322–1324.

Atsumi, K., Akiyama, T. 1975. A study of cake filtration: formulation as a Stefan problem. J. Chem. Engrg. Japan, 8, 487–492.

Auzerais, F.M., Jackson, R., Russel, W.B. 1988. The resolution of shocks and the effects of compressible sediments in transient settling. J. Fluid Mech., 195, 437–462.

Bürger, R. 2000. Phenomenological foundation and mathematical theory of sedimentation-consolidation processes. Chem. Eng. J., 80, 229–244.

Bürger, R., Bustos, M.C., Concha, F. 1999. Settling velocities of particulate systems: 9. Phenomenological theory of sedimentation processes: Numerical simulation of the transient behaviour of flocculated suspensions in an ideal batch or continuous thickener. Int. J. Mineral Process., 55, 267–282.

Bürger, R., Concha, F. 1998. Mathematical model and numerical simulation of the settling of flocculated suspensions. Int. J. Multiphase Flow, 24, 1005–1023.

Bürger, R., Concha, F. 2000. Settling velocities of particulate systems: 12. Batch centrifugation of flocculated suspensions, Preprint 2000/11, Sonderforschungsbereich 404, University of Stuttgart.

Bürger, R., Concha, F., Tiller, F.M. 2000a. Applications of the phenomenological theory to several published experimental cases of sedimentation processes. Chem. Eng. J., 80, 139–154.

Bürger, R., Evje, S., Karlsen, K.H. 2000b. On strongly degenerate convection-diffusion problems modeling sedimentation-consolidation processes. J. Math. Anal. Appl., 247, 517–556.

Bürger, R., Karlsen, K.H. 2000a. On some upwind finite difference schemes for the phenomenological sedimentation-consolidation model. Preprint 2000/05, Sonderforschungsbereich 404, University of Stuttgart.

Bürger, R., Karlsen, K.H. 2000b. A strongly degenerate convection-diffusion problem modeling centrifugation of flocculated suspensions. Submitted for publication in the proceedings volume of *Hyp 2000*.

Bürger, R., Karlsen, K.H. 2000c. A free boundary problem of a strongly degenerate convection-diffusion equation modeling pressure filtration, in preparation.

Bürger, R., Tory, E.M. 2000. On upper rarefaction waves in batch settling. Powder Technol., 108, 74–87.

Bürger, R., Wendland, W.L., Concha, F. 2000c. Model equations for gravitational sedimentation-consolidation processes. Z. Angew. Math. Mech., 80, 79–92.

Buscall, R., White, L.R. 1987. On the consolidation of concentrated suspensions, Part 1: The theory of sedimentation. J. Chem. Soc. Faraday Trans. I, 83, 873–891.

Bustos, M.C., Concha, F., Bürger, R., Tory, E.M., 1999. Sedimentation and Thickening: Phenomenological Foundation and Mathematical Theory, Kluwer Academic Publishers, Dordrecht, The Netherlands.

Concha, F., Bascur, O. 1977. Phenomenological model of sedimentation. Proceedings of the *12th International Mineral Processing Congress (XII IMPC)*, São Paulo, Brazil, vol.4, 29–46.

Concha, F., Bustos, M.C. 1986. Theory of sedimentation of flocculated fine particles. In: Moudgil, B.M. and Somasundaran, P. (eds.), Proceedings of the Engineering Foundation Conference on Flocculation, Sedimentation and Consolidation, Sea Island, GA; AIChE, New York, 275–284.

Concha, F., Bustos, M.C., Barrientos, A. 1996. Phenomenological theory of sedimentation, Chapter 3 in Tory, E.M. (ed.), Sedimentation of Small Particles in a Viscous Fluid, Computational Mechanics Publications, Southampton, UK, pp. 51–96.

Darcy, H. 1856. Les Fontaines Publiques de la Ville de Dijon. Dalmont, Paris.

Espedal, M.S., Karlsen, K.H. 2000. Numerical solution of reservoir flow models based on large time step operator splitting algorithms. In: Fasano, A., van Duijn, H. (eds.), Filtration in Porous Media and Industrial Applications. Lecture Notes in Mathematics, Springer Verlag, Berlin, to appear.

Evje, S., Karlsen, K.H. 2000. Monotone difference approximations of BV solutions to degenerate convection-diffusion equations. Siam J. Numer. Anal., 37, 1838–1860.

Font, R., Hernández, A. 2000. Filtration with sedimentation: application of Kynch's theorems. Sep. Sci. Technol., 35, 183–210.

França, S.C.A. 2000. Equações constitutivas para a sedimentação de suspensões floculentas. Doctoral Thesis, Federal University of Rio de Janeiro, Brazil.

Garrido, P., Bürger, R., Concha, F. 2000. Settling velocities of particulate systems: 11. Comparison of the phenomenological sedimentation-consolidation model with experimental results. Int. J. Mineral Process., to appear.

Holdich, R.G. 1990. Solids concentration and pressure profiles during compressible cake filtration. Chem. Eng. Comm., 91, 255–268.

Karlsen, K.H., Risebro, N.H. 2000. Convergence of finite difference schemes for viscous and inviscid conservation laws with rough coefficients. Preprint, University of Bergen.

La Heij, E.J., Kerkhof, P.J.A.M., Herwijn, A.J.M., Coumans, W.J. 1996. Fundamental aspects of sludge filtration and expression. Wat. Res., 30, 697–703.

Landman, K.A., Russel, W.B. 1993. Filtration at large pressures for strongly flocculated suspensions. Phys. Fluids A, 5, 550–560.

Landman, K.A., Sirakoff, C., White, L.R. 1991. Dewaterung of flocculated suspensions by pressure filtration. Phys. Fluids A, 3, 1495–1509.

Landman, K.A., White, L.R. 1994. Solid/liquid separation of flocculated suspensions. Adv. Colloid Interface Sci., 51, 175–246.

Lu, W.M., Tung, K.L., Pan, C.H., Hwang, K.J. 1998. The effect of particle sedimentation on gravity filtration. Sep. Sci. Technol., 33, 1723–1746.

Massarani, G. 1997. Fluidodinâmica em sistemas particulados. Editora UFRJ, Federal University of Rio de Janeiro, Brazil.

Maude, A.D., Whitmore, R.L. 1958. A generalized theory of sedimentation. Brit. J. Appl. Phys., 9, 477–482.

Richardson, J.F., Zaki, W.N. 1954. Sedimentation and fluidization I. Trans. Inst. Chem. Engrs. (London), 32, 35–53.

Rushton, A., Ward, A.S., Holdich, R.G. 2000. Solid-liquid Filtration and Separation Technology, Second Edition, Wiley-VCH, Weinheim, Germany.

Sambuichi, M., Nakakura, H., Osasa, K. 1982. The effect of gravity settling on constant pressure filtration. Mem. Fac. Engrg. Yamaguchi Univ., 33, 65–70.

Shen, C., Russel, W.B., Auzerais, F. 1994. Colloidal gel filtration: experiment and theory. AIChE J., 40, 1876–1891.

Shirato, M., Sambuichi, M., Kato, H., Aragaki, H. 1969. Internal flow mechanism in filter cakes. AIChE J., 15, 405–409.

Sis, H., Chander, S. 2000. Pressure filtration of dispersed and flocculated alumina slurries. Minerals & Metallurgical Process. 17, 41–48.

Sørensen, P.B., Moldrup, P., Hansen, J.A. 1996. Filtration and expression of compressible cakes. Chem. Eng. Sci., 51, 967–979.

Stamatakis, K., Tien, C. 1991. Cake formation and growth in cake filtration. Chem. Eng. Sci., 46, 1917–1933.

Tiller, F.M., Crump, J.R, Ville, F. 1980. A revised approach to the theory of cake filtration. In: Somasundaran, P. (ed.), Proc. of the Int. Symp. on Fine Particles Processing, vol. 2, Amer. Inst. Min., Met. Petr. Engrg., New York, 1549–1582.

Tiller, F.M., Horng, L. 1983. Hydraulic deliquoring of compressible filter cakes. AIChE J., 29, 297–305.

Tiller, F.M., Hsyung, N.B. 1995. Unifying the theory of thickening, filtration and centrifugation. Wat. Sci. Tech., 28, 1–9.

Tiller, F.M., Hsyung, N.B., Cong, D.Z. 1995. Role of porosity in filtration: XII. Filtration with sedimentation. AIChE J., 41, 1153–1164.

Tiller, F.M., Hsyung, N.B., Shen, Y.L., Chen, W. 1991. CATSCAN analysis of sedimentation and constant pressure filtration. Proceedings of the V World Congress on Filtration, Société Française de Filtration, Nice, France, vol. 2, 80–85.

Tiller, F.M., Kwon, J.H. 1998. Role of porosity in filtration: XIII. Behavior of highly compactible cakes. AIChE J., 44, 2159–2167.

Tiller, F.M., Leu, W.F. 1980. Basic data fitting in filtration. J. Chin. Inst. Chem. Engrs., 11, 61–70.

Tiller, F.M., Lu, R., Kwon, J.H., Lee, D.J. 1999. Variable flow rate in compactible filter cakes. Wat. Res., 33, 15–22.

Tiller, F.M., Yeh, C.S. 1987. The role of porosity in filtration; Part XI: Filtration followed by expression. AIChE J., 33, 1241–1256.

Wakeman, R.J., Tarleton, E.S. 1999. Filtration: Equipment Selection, Modelling and Simulation, Elsevier Science, Oxford, UK.

Wells, S. 1999. Analytical modeling of cake filtration. In: Leung, W. (ed.), Advances in Filtration and Separation Technology 12, Amer. Filt. Sep. Soc., 158–165.

Zydney, A.L., Saltzman, W.M., Colton, C.K. 1989. Hydraulic resistance of red cell beds in an unstirred filtration cell. Chem. Eng. Sci., 44, 147–159.